Crystal Structures and Growth Mechanisms of Icosahedral Au@Ag Core−Shell and Au/Ag Twin Nanocrystals Prepared by PVP-Assisted N , N -Dimethylformamide Reduction

ARTICLE *in* CRYSTAL GROWTH & DESIGN · SEPTEMBER 2010

Impact Factor: 4.89 · DOI: 10.1021/cg100748g

7 AUTHORS, INCLUDING:

Masaharu Tsuji
Kyushu University
440 PUBLICATIONS **6,163** CITATIONS
SEE PROFILE

Nobuhiro Miyamae
14 PUBLICATIONS **648** CITATIONS
SEE PROFILE

Jahangir Alam
University of Rajshahi
10 PUBLICATIONS **91** CITATIONS
SEE PROFILE

DOI: 10.1021/cg100748g

CRYSTAL GROWTH & DESIGN Article

2010, Vol. 10
4085–4090

Crystal Structures and Growth Mechanisms of Icosahedral Au@Ag Core−Shell and Au/Ag Twin Nanocrystals Prepared by PVP-Assisted *N*,*N*-Dimethylformamide Reduction

Masaharu Tsuji,*[,†,‡] Masatoshi Ogino,[‡] Mika Matsunaga,[†] Nobuhiro Miyamae,[‡] Ryoichi Matsuo,[‡] Michiko Nishio,[‡] and Md. Jahangir Alam[‡]

[†]*Institute for Materials Chemistry and Engineering, Kyushu University, Kasuga 816-8580, Japan, and* [‡]*Department of Applied Science for Electronics and Materials, Graduate School of Engineering Sciences, Kyushu University, Kasuga 816-8580, Japan*

Received June 4, 2010; Revised Manuscript Received July 3, 2010

ABSTRACT: Icosahedral Au@Ag core−shell nanocrystals have been prepared using a two-step reduction method. In the first step, icosahedral Au core seeds were prepared by reducing $HAuCl_4 \cdot 4H_2O$ in tetraethylene glycol (TEG) under microwave (MW) heating in the presence of polyvinylpyrrolidone (PVP) as a polymer surfactant. In the second step, Ag shells were overgrown on icosahedral Au seeds in *N*,*N*-dimethylformamide (DMF) in the presence of PVP under oil-bath heating for 3 h or MW heating for 10 min. Crystal structures of products were characterized using TEM, TEM-EDS, and SEM. Under oil-bath heating, Au@Ag icosahedral nanocrystals nearly fully covered by Ag shells were prepared, whereas those partially covered by tetrahedral units of Ag shells were formed under MW heating. On the basis of these findings, it was concluded that icosahedral Au@Ag core−shell particles are formed through stepwise growth of tetrahedral units, as observed in the crystal growth of monometallic icosahedral Ag crystals in DMF. There were minor Au/Ag twin products under fast MW heating where icosahedral Ag nanocrystals are grown up outside of icosahedral Au cores sharing one decahedral Au core or one {111} facet of a tetrahedral unit. These findings provide new information on the stepwise growth mechanism of nanocrystals in the presence of icosahedral Au seeds in DMF.

Introduction

In recent years, bimetallic nanoparticles have received intensive attention, owing to their novel optical, electronic, magnetic, and catalytic properties, different from those of individual metals.[1−11] We have recently studied shape-selective growth of Au@Ag core−shell nanocrystals prepared using a two-step method.[12−14] First, Au nanocrystal seeds with various shapes including single-crystal octahedron, single-twinned triangular or hexagonal plate, and multiple-twinned decahedron were prepared by reducing $HAuCl_4$ in ethylene glycol (EG) in the presence of polyvinylpyrrolidone (PVP) as a polymer surfactant under microwave (MW) heating. Although these Au nanoparticles possess different shapes, a common feature is that they are mainly surrounded by {111}-type facets. Subsequently, thus-obtained Au seeds were added into either EG or *N*,*N*-dimethylformamide (DMF) solution for overgrowth of Ag shells by MW heating or oil-bath heating. Here EG and DMF act as both solvent and reductant. Transmission electron microscope (TEM) and TEM−energy dispersed X-ray spectroscopic (EDS) observations demonstrated that shapes of formed Ag shells strongly depend on both shapes of initial Au seeds and solvent. Cubic, triangular-bipyramidal, and rod/wire Ag shells with {100}-type dominant facets were epitaxially formed over octahedral, triangular platelike, and decahedral Au core seeds in EG, respectively, whereas the same shapes as those of Au cores with {111}-type facets were overgrown on Au core seeds in DMF. Our studies reveal that it is possible to controllably prepare the Au@Ag core/shell nanocrystal structures with optional uniform crystalline planes by the same Au seed source and different reaction solvent and reductant. Although Au@Ag core−shell nanocrystals using octahedral, triangular-plate-like, and decahedral particles have been reported, no studies have been carried out using a multiple-twin icosahedral Au core as seeds.

We have recently studied stepwise growth of decahedral and icosahedral silver nanocrystals in DMF.[15] Besides decahedral and icosahedral nanoparticles, a series of their intermediate particles, which consist of a combination of two or more tetrahedra, are obtained. It was found that decahedral and icosahedral nanoparticles are not formed through assembling of tetrahedra formed separately but are produced through the stepwise growth of tetrahedral units on specific facets in DMF. A simple combination model of tetrahedral units suggested that the growth position of the fourth tetrahedral unit determines whether a decahedron or icosahedron is finally produced (Figure 1). The growth of the fourth tetrahedral unit on the 3a facet leads to a decahedron, while that on 3b or 3c gives an icosahedron.

In the present study, we attempted to prepare novel icosahedral Au@Ag nanocrystals in high yield by a two step method. In the first step, icosahedral Au core crystals were prepared in tetrathylene glycol (TEG) in high yield under MW heating. Then, Ag shells were overgrown on icosahedral Au core seeds in DMF under oil-bath heating for 3 h or MW heating for 10 min. Since the same shapes of Ag shells were formed over Au cores in DMF for octahedral, triangular plate-like, and decahedral Au core seeds, new icosahedral Au@Ag nanocrystals are expected to be formed using icosahedral Au particles as cores. If we succeed in the preparation of icosahedral Au@Ag nanocrystals in DMF, it is interesting to examine whether icosahedral Ag shells are epitaxially

*To whom correspondence should be addressed: E-mail: tsuji@cm.kyushu-u.ac.jp.

Published on Web 07/20/2010

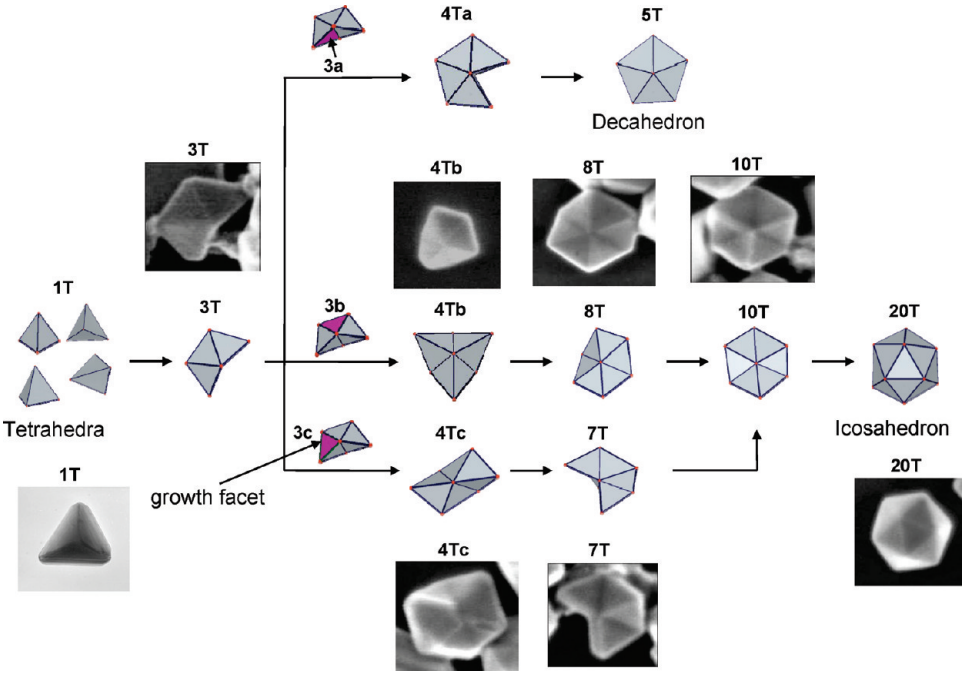

Figure 1. Stepwise growth of decahedral and icosahedral Ag nanocrystals in DMF.[15] *n*T implies that particles consist of a combination of *n* numbers of tetrahedra.

formed on Au cores via stepwise growth as shown in Figure 1 or via uniform growth in the presence of icosahedral Au cores. This result gives information on the roles of icosahedral Au cores in the formation of icosahedral Ag shells. We found here that different shapes of Ag shells are formed under long oil-bath heating and short MW heating. Core−shell particles are produced under oil-bath heating. On the other hand, besides core−shell crystals, new Au and Ag twin nanocrystals are grown up sharing one decahedral Au core or one {111} facet of a tetrahedral unit under MW heating. The growth mechanisms of each nanocrystal under oil-bath heating and MW heating are discussed.

Experimental Section

Icosahedral Au@Ag core−shell nanocrystals were prepared using a two-step reduction method. In our experiments, TEG and DMF were used as both reductant and solvent. As a first step, Au nanocrystal seeds were prepared by MW heating in TEG. In the process, 245 mg of $HAuCl_4 \cdot 4H_2O$ was dissolved in 30 mL of TEG solvent to prepare a 2.4 mM $HAuCl_4 \cdot 4H_2O$ solution. Then, 500 mM PVP (M_w = 40k in terms of monomeric units) was added into the above solution. The whole reaction system was heated for 5 min by MW irradiation in a continuous wave mode (Shikoku Keisoku: μ Reactor: 700 W). The solution temperature increased to 220 °C after heating the solution for about 2 min, and it was kept at this temperature for about 3 min. After naturally cooling down to room temperature, Au seeds were separated from C_2H_5OH solution by centrifuging the colloidal solution at 15,000 rpm for 30 min three times and redispersed in a DMF solution. We used a combination of dropwise injection of $AgNO_3$ and long oil-bath heating or premixing $AgNO_3$ and low-power, short MW heating for the overgrowth of Ag shells in the second step. In the former experiment, DMF solution (14 mL) containing 536 mM of PVP (M_w = 1,300 k) was preheated at 140 °C for 30 min, and Au seeds in 1 mL of DMF solution were added to the above solution. Then, 15 mL of $AgNO_3$/DMF solution was injected dropwise to the solution using a syringe pump at an injection rate of 0.3 mL/min. The final concentrations of Au, Ag, and PVP were 1, 3, and 250 mM, respectively. After all reagents were introduced to the solution, the solution was heated in an oil bath for 3 h. In the latter experiment, Au seeds in 1 mL of DMF solution were added to 19 mL of DMF solution involving $AgNO_3$ and PVP. The final concentrations of Au, Ag, and PVP were the same as those of the first experiment. The solution was heated under MW irradiation (100 W) for 10 min. The solution temperature increased to a boiling point of 153 °C after MW heating for about 2 min, and it was kept at this temperature for about 8 min.

Au and Au@Ag products were obtained from C_2H_5OH solution by centrifuging the colloidal solution at 15,000 rpm for 30 min three times for TEM (JEOL JEM-2000XS) and SEM (Hitachi S-4800) observations. TEM-EDS (JEOL 2100F) data were also measured. Extinction spectra of the product solutions were measured in the UV−visible (vis) region using a Shimadzu UV-3600 spectrometer.

Results and Discussion

Preparation of Icosahedral Au Seeds. In our previous experiments using EG as both solvent and reductant, mixtures of octahedral, triangular-plate-like, and decahedral particles were prepared under MW heating.[12,14,16] By the addition of NaCl to the $HAuCl_4 \cdot 4H_2O$/PVP/EG solution, icosahedral particles were obtained besides the above shapes of Au nanocrystals.[16c,d] However, the yield of icosahedral Au particles was not sufficiently high to obtain Au@Ag nanocrystals in high yield. In the present study, at first we attempted to find optimum experimental conditions for the preparation of icosahedral Au seeds by changing various experimental parameters, such as concentrations of reagent and PVP, solvent and reductant (EG, diethylene glycol, and TEG), MW power, and heating time. Then we found that MW heating of reagent solution in TEG at 700 W was best for the preparation of icosahedral Au nanocrystals in high yield.

Parts a and b of Figure 2 show TEM and SEM images of products obtained in TEG under MW heating. Major products were multiple-twin icosahedral nanocrystals with an average size of 88 ± 13 nm, and their yield was 93%. The definition of particle size of icosahedra used in this study is shown in Figure 2c. Here the yield was determined by counting the total numbers of icosahedral Au particles and evaluating their fraction in all products. In addition, small

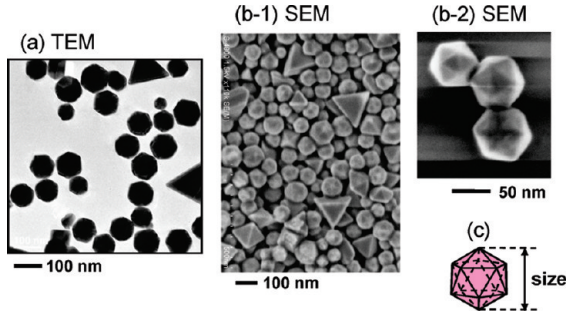

Figure 2. TEM and SEM images of Au core nanocrystals prepared from the $HAuCl_4 \cdot 4H_2O$ (2.4 mM)/PVP (40k, 500 mM)/TEG mixture under MW heating at 700 W for 5 min.

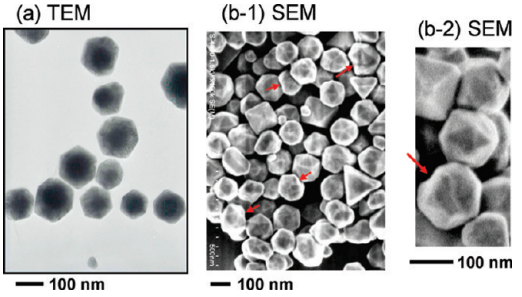

Figure 3. TEM and SEM images of the Au@Ag nanocrystals prepared in the Au seeds/$AgNO_3$/PVP(1,300 K)/DMF mixture by oil-bath heating at 140 °C for 3 h.

amounts of single-crystal octahedral particles (2%), single-twin triangular-plate-like particles (3%), and five-twin decahedral particles (2%) were obtained. It is clear from TEM and SEM images that nearly perfect icosahedral Au nanocrystals having twin-lines in SEM images are prepared.

Preparation of Icosahedral Au@Ag Crystals under Oil-Bath Heating. Parts a and b of Figure 3 show TEM and SEM images of Au@Ag particles obtained by dropwise injection of $AgNO_3$/DMF solution to icosahedral Au seeds/PVP-(1,300 k)/DMF solution, with heating at 140 °C for 3 h. In Figure 3a, black contrast Au cores are covered by bright contrast Ag shells in all cases. Most of the product particles are icosahedral shapes (yield 88%). This shows that the same icosahedral shape of Ag shells with {111} facets is formed from icosahedral Au cores with {111} facets in DMF. This result is consistent with our previous findings for other shapes of Au@Ag particles, where the same shapes of Ag shells having {111} facts were grown in DMF.[13] The average size of icosahedral Au@Ag particles was 147 ± 22 nm, indicating that ≈30 nm Ag shells are overgrown on icosahedral Au cores. In some icosahedral Au@Ag particles, icosahedral Ag shells are not fully grown on icosahedral Au cores. In such cases, product Au@Ag particles have notches, as shown by red arrows in Figure 3b-1 and b-2.

In order to obtain more information on crystal structures of icosahedral Ag@Au particles, TEM-EDS measurements of product particles were carried out (Figure 4a−d). It is clear from these data that all Au@Ag core−shell nanocrystals consist of Au cores and Ag shells. The distributions of the Au and Ag components along diagonal lines A and B in Figure 4b are shown in Figure 4e and f, respectively. The distribution of the Ag component is nearly symmetric for most product particles, as shown in Figure 4e, indicating that uniform icosahedral Ag shells are overgrown in such particles. On the other hand, the distributions of the Ag component for some particles are asymmetric (e.g., two particles along line B in Figure 4b), as shown in Figure 4f, due to incomplete growth of icosahedral shells. The appearance of notch and asymmetric Ag distributions indicates that icosahedral Au@Ag nanocrystals are grown via stepwise growth of truncated tetrahedral units.

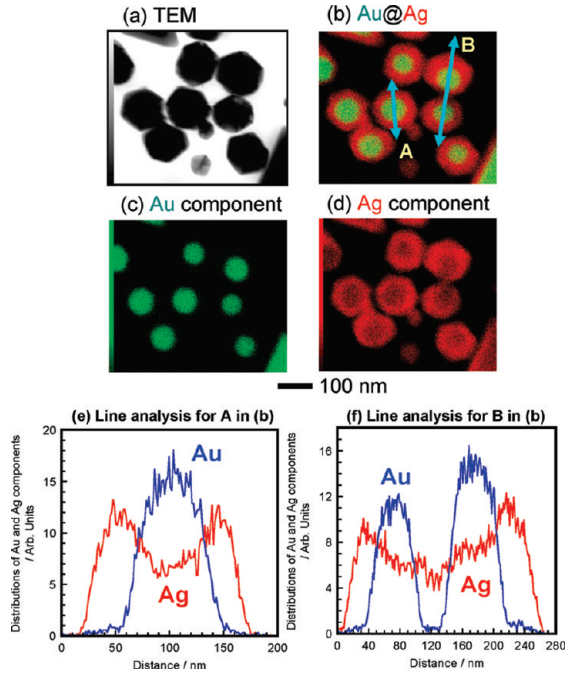

Figure 4. (a) TEM, (b−d) TEM-EDS, and (e and f) line analysis data of the Au@Ag nanocrystals prepared from the Au seeds/$AgNO_3$/PVP(1,300k)/DMF mixture under oil-bath heating for 3 h.

In order to further examine the growth mechanism in oil-bath heating, TEM and TEM-EDS were measured for products obtained just after complete injection of reagent to DMF (50 min just after starting injection). The results obtained are given in Figure 5a−d, and line analysis data for a typical particle in Figure 5b are shown in Figure 5e. Most product particles are highly asymmetric, and the distribution of the Ag component is also asymmetric, as shown in Figure 5e. It was therefore concluded that the Au@Ag particles obtained in Figure 5 are intermediate particles of icosahedral Au@Ag nanocrystals in earlier stages than those in Figure 4. After slow reduction of Ag^+ during heating at 140 °C for a further 3 h, icosahedral Au@Ag nanocrystals having a more symmetrical Ag shell component are formed in DMF.

Preparation of Icosahedral Au@Ag Crystals under Microwave Heating. We have synthesized an Ag shell over icosahedral Au core particles under short MW heating at a higher temperature without using a syringe pump to examine the effects of the heating rate, the solution temperature, and the concentration of Ag^0. If $AgNO_3$ was heated rapidly, rapid reduction of Ag^+ to Ag^0 occurred. In such a case, the $[Ag^0]$ concentration exceeds supersaturation of $[Ag^0]$, and Ag particles are formed via a homogeneous process and the yield of Au@Ag particles becomes low. In order to suppress such supersaturation of $[Ag^0]$, an Ag^+ solution was heated under low-power MW irradiation (100 W).

Parts a and b of Figure 6 show TEM and SEM images of product particles obtained under MW irradiation. TEM-EDS and their line analysis data for some typical particles are

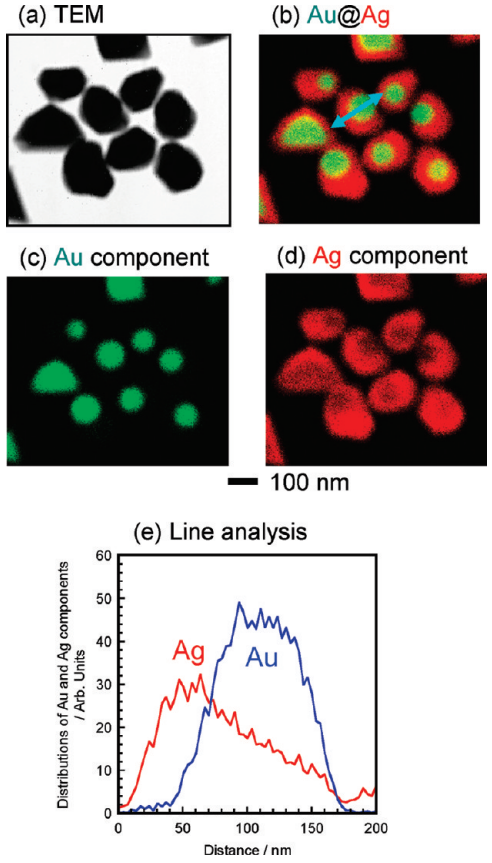

Figure 5. (a) TEM, (b−d) TEM-EDS, and (e) line analysis data of the Au@Ag nanocrystals prepared from the Au seeds/$AgNO_3$/PVP(1,300 k)/DMF mixture obtained just after injection of all reagents, and (e) line analysis data for a particle shown in part b.

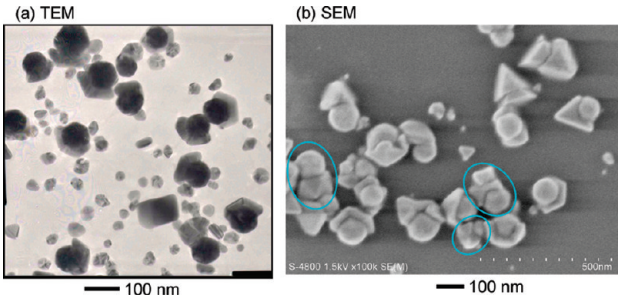

Figure 6. (a) TEM and (b) SEM data of the Au@Ag nanocrystals prepared from the Au seeds/$AgNO_3$/PVP(1,300 k)/DMF mixture under MW heating for 10 min.

shown in Figure 7. It should be noted that the shapes of the products are significantly different from those obtained under a long oil-bath heating. In most cases, icosahedral Au cores are partially capped by Ag shells, which correspond to intermediates of icosahedral Ag particles. In most cases, icosahedral Au core particles of ≈80 nm average size are partially covered by ≈30 nm Ag shells in thickness. The Ag shell consists of a combination of 2−5 teterahedral units which correspond to the early stages of intermediates of icosahedra (see Figure 1).

It should be noted that there exist some Au/Ag bimetallic particles where icosahedral Ag nanocrystals are grown up outside of icosahedral Au cores, as shown by blue circles in Figures 6b and 7b. The detailed crystal structures and their growth mechanisms of these nanocrystals will be shown in the next section. Parts e and f of Figure 7 show line analysis data of particles A and B shown in Figure 7b. It is clear from these data that nearly the same sizes of icosahedral Ag particles are formed and Au cores are covered by thin Ag shells. Although particle A is a twin Au/Ag icosahedral crystal, the Ag component of particle B does not consist of a perfect icosahedron due to lack of some tetrahedra.

Crystal Structures and Growth Mechanisms of Icosahedral Au@Ag Nanocrystals. We have recently found that icosahedral Ag nanocrystals are formed via stepwise growth of tetrahedral units (Figure 1).[15] The most outstanding finding in this study is that icosahedral Ag shells are grown via a similar stepwise process even in the presence of icosahedral Au seeds. According to the general heterogeneous nucleation and growth theory,[5,17] the growth mode is mainly determined by the lattice match and interactions between the overlayer and substrate. Three types of growth processes are proposed when a substance is deposited on a substrate in the gas phase: the layered growth (Frank−van der Merwe (F-M) type), the island growth (Volmer−Weber (V−W) type), and the intermediate type of growth (Stranski−Krastanow (S−K) type). These models can also be applicable to the heterogeneous epitaxial growth of an Ag shell over an Au core observed in this study in the liquid phase. According to the above models, the following three mechanisms are possible for the formation of icosahedral Au@Ag nanocrystals (Figure 8). The first case is uniform layered growth of an icosahedral Ag shell over an Au core via F-M type growth (a-1). The second case is the island growth of Ag shells in all 20 facets via V−W type growth (a-2). The third case is the intermediate type of growth via S−K type growth (a-2). In this case, a monolayer or bilayer of an Ag shell is initially formed and then island growth occurs over thin Ag layers. On the basis of TEM, TEM-EDS, and SEM observations, it was found that icosahedral Ag shells are not grown through the above three types, because a truncated tetrahedral unit of an Ag shell is initially formed on one specific {111} facet of the icosahedral Au core and then stepwise growth of a tetrahedral unit of Ag shell layers occurs from the first unit to all 20 {111} facets of Au icosahedra. This mechanism is shown as type (b-1) in Figure 9.

In a long oil-bath heating in DMF, Ag^+ is slowly reduced. Under such conditions, the Ag concentration is lower than the point of supersaturation. Below supersaturation, homogeneous nucleation of Ag particles in solution cannot take place, so that only heterogeneous nucleation on the Au core and stepwise growth of Ag shell units can take place. Ag^+ is reduced more rapidly under short MW heating at higher temperature. In this case, the concentration of Ag^0 is locally higher than the point of supersaturation; not only heterogeneous nucleation on Au cores, as observed in oil-bath heating but also homogeneous nucleation of Ag particles, leading to Ag particles occurs. Actually the formation of small Ag particles by homogeneous nucleation of Ag particles was observed (Figures 6a and 7a). When we carefully analyzed the TEM-EDS data of Au@Ag particles under MW irradiation, we found that thin Ag layers are fully overgrown on Au icosahedrons (Figure 7a and b). The atomic ratio of the Ag component in Au@Ag particles covered by thin Ag layers was only 3−4% (e.g., within the red circles in Figure 7b). Thus, although the major route to icosahedral Au@Ag particles is type b-1 stepwise growth, uniform covering of thin Ag shells on Au cores also occurs under rapid MW heating.

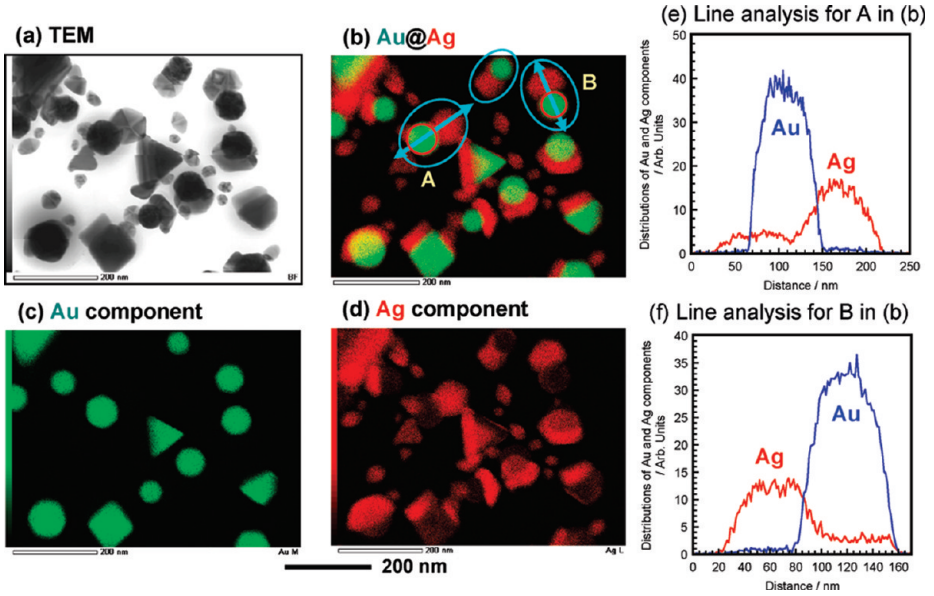

Figure 7. (a) TEM, (b−d) TEM-EDS, and (e and f) line analysis data of the Au@Ag nanocrystals prepared from the Au seeds/$AgNO_3$/PVP(1,300 k)/DMF mixture under MW heating for 10 min. The Ag/Ag atomic ratios within red circles in Figure 7b were measured to be 3−4:96−97, respectively.

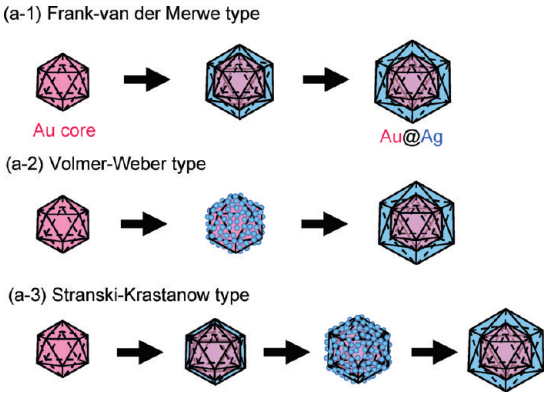

Figure 8. Possible growth mechanisms of icosahedral Au@Ag nanocrystals.

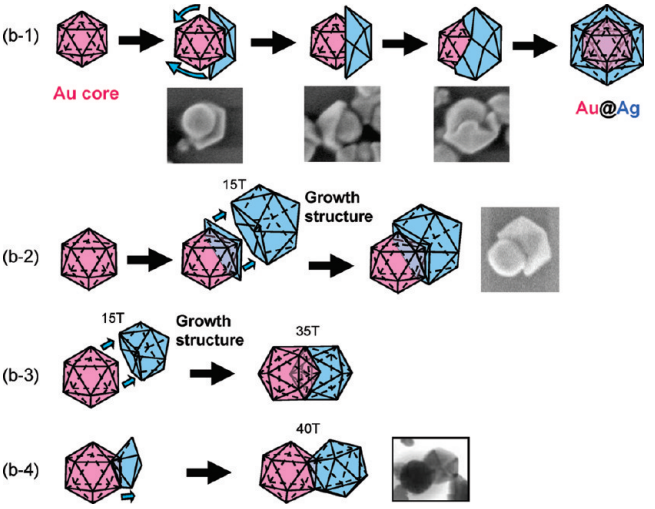

Figure 9. Possible stepwise growth mechanisms of icosahedral Au@Ag nanocrystals in DMF under MW heating. Blue arrows are the growth direction of truncated tetrahedra in b-1 and of tetrahedral units in b-2, b-3, and b-4.

It should be noted that other shapes of Au@Ag icosahedrons are also formed under MW heating, as shown by blue circles in Figures 6 and 7. In these cases, after nucleation and formation of one tetrahedral unit on an icosahedral Au core, crystal growth occurs outside of the Au core. Then, b-2 and b-4 types of icosahedral Au@Ag particles are produced. In the formation of the b-2 type of icosahedral particles, a truncated tetrahedral Ag shell unit is initially formed over a decahedral unit of an icosahedral Au core and an icosahedral Ag shell is overgrown, sharing the same Au decahedral particles in the center part. Since the lattice constant of Au (0.4079 nm) is close to that of Ag (0.4086 nm), the direct formation of tetrahedral Ag units over a decahedral unit of an icosahedral Au core is possible. In this case, the formation of a combined icosahedral particle (b-3 type in Figure 9) is expected, where the sizes of two Au and Ag icosahedral particles will be nearly the same because of close matching of the lattice constants of Au and Ag. When we looked for b-2 and b-3 types of twin particles in TEM and SEM images, the sizes of the outer Ag shells are always larger than those of the icosahedral Au cores. This indicates that only the b-2 type of Au@Ag particle is formed sharing the same Au decahedral unit. Besides b-1 and b-2 types of Au@Ag nanocrystals, the b-4 type of twin Au/Ag nanocrystal is observed. Since the sizes of Au and Ag icosahedral crystals are nearly the same, an Ag tetrahedral unit is initially grown on an icosahedral Au particle and an icosahedral Au/Ag twin crystal is formed via stepwise growth of tetrahedral units (Figure 1). The yields of b-1/b-2/b-4 types of particles under MW heating were 70:25:5, respectively. The growth direction of each type of crystal is shown by blue arrows in Figure 9. The b-1 type of crystal is grown along the surface to form an icosahedral Ag shell, whereas b-2 and b-4 types of crystals grow up perpendicularly from the surface to form a new icosahedral Ag crystal, sharing the same decahedron or a {111} facet. The high yield of the former type under MW heating suggests that the b-1 type of Au@Ag crystal is the most favorable structure even in the rapid MW heating.

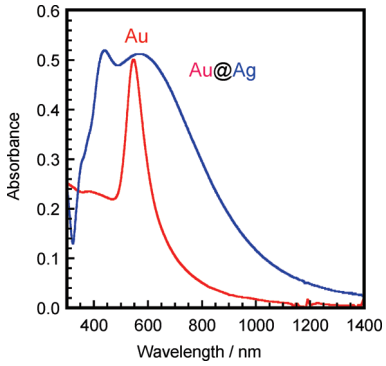

Figure 10. UV−vis spectra of icosahedral Au core particles prepared under MW heating and Au@Ag core−shell particles prepared under oil-bath heating.

When b-1 and b-2 types of icosahedral Au@Ag crystals are formed, ABC layers of Ag fcc facets are initially overgrown on ABC layers of Au facets. On the other hand, for the formation of the b-4 type of icosahedral Au/Ag twin crystals, CBA layers of the Ag shell are initially created on ABC layers of the Au core, leading to the formation of a twin plane between Au and Ag icosahedra. It is generally known that the probability of twinning increases with increasing concentration of atoms.[18] A higher Ag^0 concentration under MW heating will be one of the key factors for the formation of Au/Ag icosahedral twin particles, even though the yield of the b-4 type of twin crystal is only 5%.

UV−vis Spectra. Under oil-bath heating, icosahedral Au@Ag particles are prepared in high yield. In order to characterize the optical properties of icosahedral Au@Ag nanocrystals, UV−vis extinction spectra were measured. Figure 10 shows UV−vis extinction spectra of icosahedral Au core and Au@Ag core shell nanocrystals obtained at an $[AgNO_3]/[HAuCl_4]$ molar ratio of 3. The absorption spectrum of an icosahedral Au core solution exhibits a sharp surface plasmon resonance (SPR) peak in the 500−800 nm region with a peak at ≈550 nm, being consistent with the reported data.[19,20] The spectrum of Au@Ag gives a more broad band in the 320−1000 nm region, with obvious double peaks at ≈430 and ≈600 nm. Although observed SPR bands of Ag nanoparticles depend on their shape and size, they are generally observed in the wavelength range of 320−800 nm with a peak at ≈420 nm.[21] The peaks of Au@Ag at ≈430 nm and ≈600 nm can be attributed to the SPR band of the Ag shell and Au core components of an icosahedron, respectively.

Conclusion

Icosahedral Au@Ag core−shell nanocrystals have been prepared in high yield by using a two-step method. In the first step, icosahedral Au core nanocrystals with {111} facets were prepared by a MW-polyol method in TEG in the presence of PVP (M_w = 40 k). As a second step, when Ag^+ was reduced by using these Au nanocrystals as seeds in PVP (M_w = 1,300 k)/DMF with oil-bath or MW heating, icosahedral Au@Ag core−shell nanocrystals and various shapes of their intermediates were formed. TEM, TEM-EDS, and SEM data indicated that icosahedral Au@Ag nanocrystals are grown via stepwise growth of icosahedral shells which consist of combinations of truncated tetrahedral units. Combination of this finding with our previous result that icosahedral Ag nanocrystals are grown via stepwise growth of tetrahedral units led us to conclude that icosahedral Au@Ag core−shell nanocrystals are also produced via a stepwise process even in the presence of icosahedral Au seeds. Under a short MW irradiation at higher temperature, twin Au/Ag particles are formed from icosahedral Au seeds. These observations give new information on crystal growth of bimetallic particles using multiple-twin core seeds. To understand the stepwise-growth mechanism of icosahedral Au@Ag nanocrystals in DMF, further detailed studies including theoretical calculations will be required.

Acknowledgment. We thank Prof. Hiroki Ago for the use of his SEM. This work was supported by a Grant-in-Aid for Scientific Research (B) from the Ministry of Education, Culture, Sports, Science, and Technology of Japan (No. 22310060).

References

(1) Toshima, N. *Pure Appl. Chem.* **2000**, *72*, 317.
(2) Hodak, J.; Henglein, A.; Giersig, M.; Hartland, G. V. *J. Phys. Chem. B* **2000**, *104*, 11708.
(3) Nadagouda, M. N.; Varma, R. S. *Cryst. Growth Des.* **2007**, *7*, 2582.
(4) Habas, S. E.; Lee, H.; Radmilovic, V.; Somorjai, G. A.; Yang, P. *Nat. Mater.* **2007**, *6*, 692.
(5) Fan, F.-R.; Liu, D.-Y.; Wu, Y.-F.; Duan, S.; Xie, Z.-X.; Jiang, Z.-Y.; Tain, Z.-Q. *J. Am. Chem. Soc.* **2008**, *130*, 6949.
(6) Wu, Y.; Jiang, P.; Jiang, M.; Wang, T,-W.; Chuan-Fei Guo, X.-F.; Xie, S.-S.; Wang, Z.-L. *Nanotechnology* **2009**, *20*, 305602 (10 pp).
(7) Zhang, H. T.; Ding, J.; Chow, G. M.; Ran, M.; Yi, J. B. *Chem. Mater.* **2009**, *21*, 5222.
(8) (a) Hu., J.-W.; Li, J.-F.; Ren, B.; Wu, D.-Y.; Sun, S.-G.; Tian, Z.-Q. *J. Phys. Chem. C* **2007**, *111*, 1105. (b) Deng, S.; Pingali, K. C.; Rockstraw, D. A. *IEEE Sens. J.* **2008**, *8*, 730. (c) Yang, Y.; Shi, J.; Kawamura, G.; Nogami, M. *Scr. Mater.* **2008**, *58*, 862.
(9) Majo, K. J.; De, C.; Obare, S. O. *Plasmonics* **2009**, *4*, 61.
(10) (a) Tsuji, M.; Hikino, S.; Sano, Y.; Horigome, M. *Chem. Lett.* **2009**, *38*, 518. (b) Tsuji, M.; Hikino, S.; Tanabe, R.; Sano, Y. *Chem. Lett.* **2009**, *38*, 860. (c) Tsuji, M.; Hikino, S.; Tanabe, R.; Yamaguchi, D. *Chem. Lett.* **2010**, *39*, 334.
(11) Tsuji, M. Core Shell Particles. In *Shape and Structure Control of Metal Nano- and Fine-particles*; Yonezawa, T., Ed.; CMC: Tokyo, 2009; p 166 (in Japanese).
(12) Tsuji, M.; Miyamae, N.; Lim, S.; Kimura, K.; Zhang, X.; Hikino, S.; Nishio, M. *Cryst. Growth Des.* **2006**, *6*, 1801.
(13) Tsuji, M.; Matsuo, R.; Jiang, P.; Miyamae, N.; Ueyama, D.; Nishio, N.; Hikino, S.; Kumagae, H.; Kamarudin, K. S. N.; Tang, X.-L. *Cryst. Growth Des.* **2008**, *8*, 2528.
(14) Tsuji, M.; Nishio, M.; Jiang, P.; Miyamae, N.; Lim, S.; Matsumoto, K.; Ueyama, D.; Tang, X. *Colloid Surf., A* **2008**, *317*, 247.
(15) Tsuji, M.; Ogino, M.; Matsuo, R.; Kumagae, H.; Hikino, S.; Kim, T.; Yoon, S.-H. *Cryst. Growth Des.* **2010**, *10*, 296.
(16) (a) Tsuji, M.; Hashimoto; Nishizawa, Y.; Tsuji, T. *Chem. Lett.* **2003**, *32*, 1114. (b) Tsuji, M.; Hashimoto, M.; Nishizawa, Y.; Kubokawa, M.; Tsuji, T. *Chem.—Eur. J.* **2005**, *11*, 440. (c) Tsuji, M.; Miyamae, N.; Hashimoto, M.; Nishio, M.; Hikino, S.; Ishigami, N.; Tanaka, I. *Colloid Surf., A* **2007**, *302*, 587. (d) Tsuji, M.; Miyamae, N.; Nishio, M.; Hikino, S.; Ishigami, N. *Bull. Chem. Soc. Jpn.* **2007**, *80*, 2024.
(17) Venables, J. *Introduction to Surface and Thin Film Processes*; Cambridge University Press: Cambridge, 2000.
(18) (a) Jagannathan, R. *J. Imaging Sci.* **1991**, *35*, 103. (b) Jagannathan, R.; Gokhale, V. V. *J. Imaging Sci.* **1991**, *35*, 113.
(19) Seo, D.; Yoo, C. I.; Chung, I. S.; Park, S. M.; Ryu, S.; Song, H. *J. Phys. Chem. C* **2008**, *112*, 2469.
(20) Sánchez-Iglesias, A.; Pastoriza-Santos, I.; Pérez-Juste, J.; Rodríguez-González, B.; García de Abajo, F J.; Liz-Marzán, L. M. *Adv. Mater.* **2006**, *18*, 2529.
(21) (a) Wiley, B.; Im, S.-H.; Li, Z.-Y.; McLellan, J. M.; Siekkinen, A.; Xia, Y. *J. Phys. Chem. B* **2006**, *110*, 15666. (b) Tang, X.-L.; Tsuji, M.; Nishio, M.; Jiang, P.; Jang, S.; Yoon, S.-H. *Colloid Surf., A* **2009**, *338*, 33.